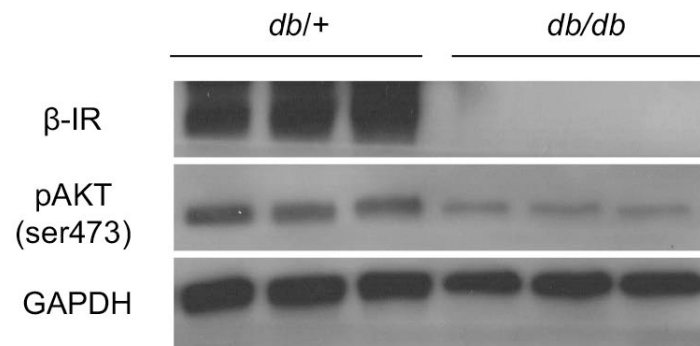
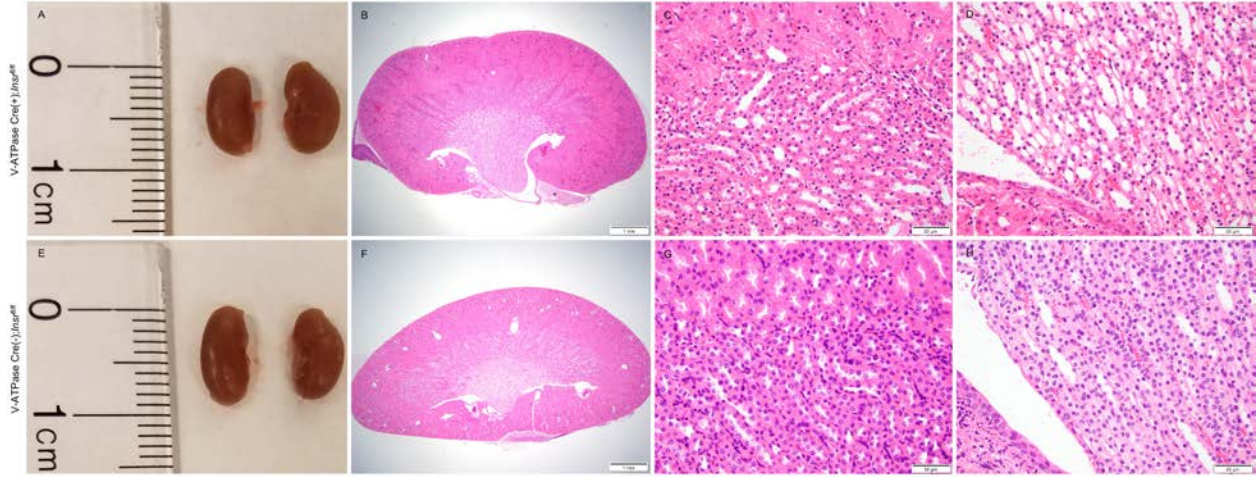


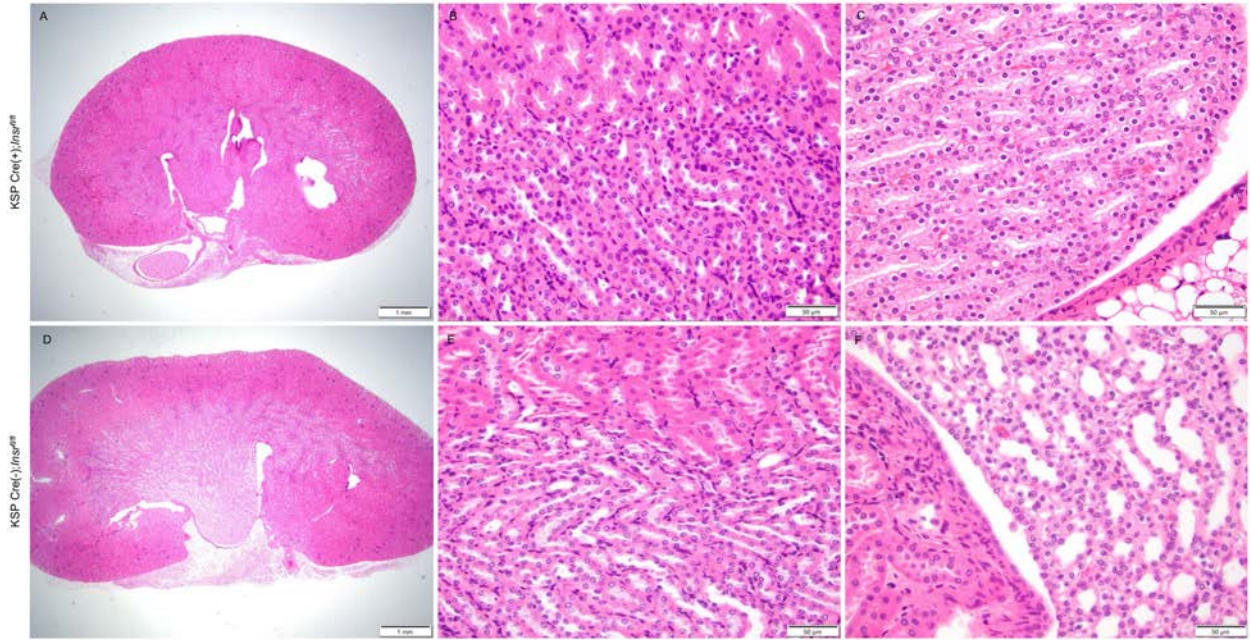
Supplemental Figures and Table Legends:



Supplemental Figure 1. Insulin receptor and PI3K/AKT activity is suppressed in diabetic mouse bladder. Representative Western blots probed for β -IR, pAKT (ser473), and GAPDH in *db/+* and *db/db* mice. Each lane depicts bladder β -IR expression and AKT phosphorylation from separate mice.

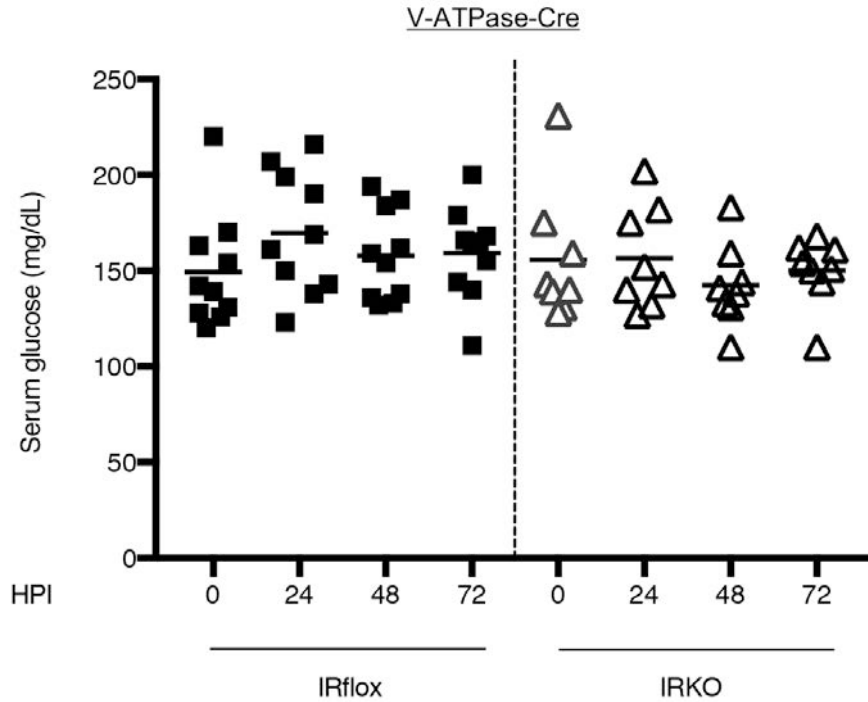


Supplemental Figure 2. Kidney histology in V-ATPase IRKO mice and littermate controls. (A/E) Macroscopic images of kidneys dissected from IRKO mice (A, top panels) and littermate controls (E, bottom panels). (B-D and F-H) Representative low and higher power micrographs of paraffin-embedded, fixed kidney tissues from IRKO mice (top panels) and littermate controls (bottom panels) stained with hematoxylin & eosin. Micrographs show total kidney (B/F, left panels), corticomedullary junction (C/G, center panels) and renal pelvis/papilla (D/H, right panels).



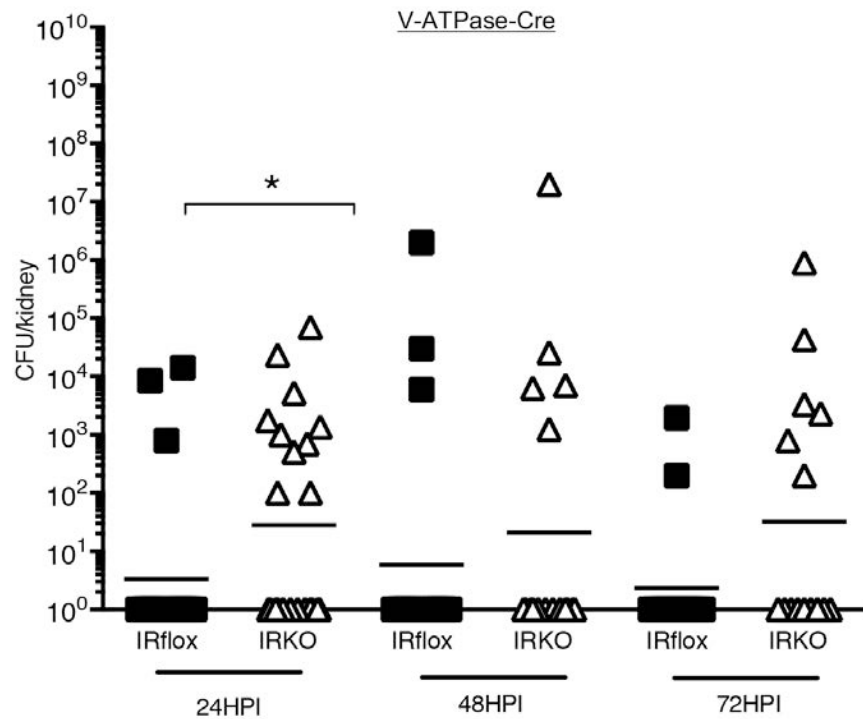
Supplemental Figure 3. Kidney histology in KSP-IRKO mice and littermate controls.

Representative low and higher power micrographs of paraffin-embedded, fixed kidney tissues from IRKO mice (top panels) and littermate controls (bottom panels) stained with hematoxylin & eosin. Micrographs show total kidney (A/D, left panels), corticomedullary junction (B/E, center panels) and renal pelvis/papilla (C/F, right panels).

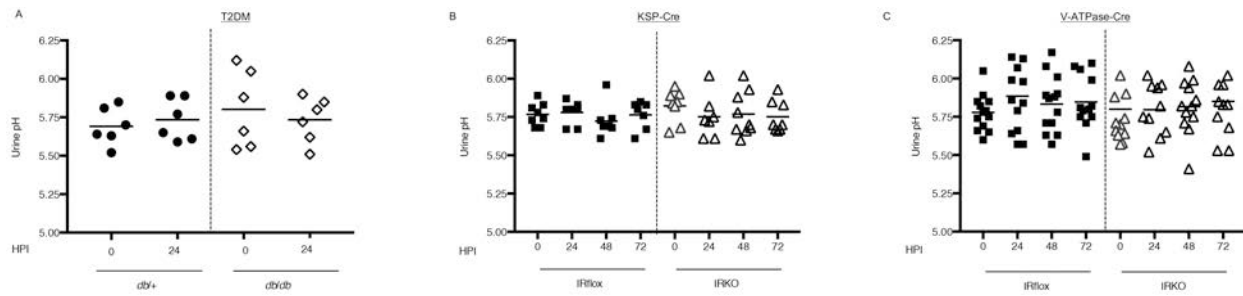


Supplemental Figure 4. Serum glucose values following experimental UTI.

Female control (squares) and IRKO mice (triangles) were subjected to experimental UTI ($n=8-10$ mice/genotype). At the indicated time points post infection, serial non-fasting serum glucose samples were measured from the same mouse. The horizontal line indicates the median of each group. Significant differences in serum glucose concentrations were not identified using a repeated measures ANOVA with Dunn's multiple comparisons test. These data supplement the findings in **Table 2**.

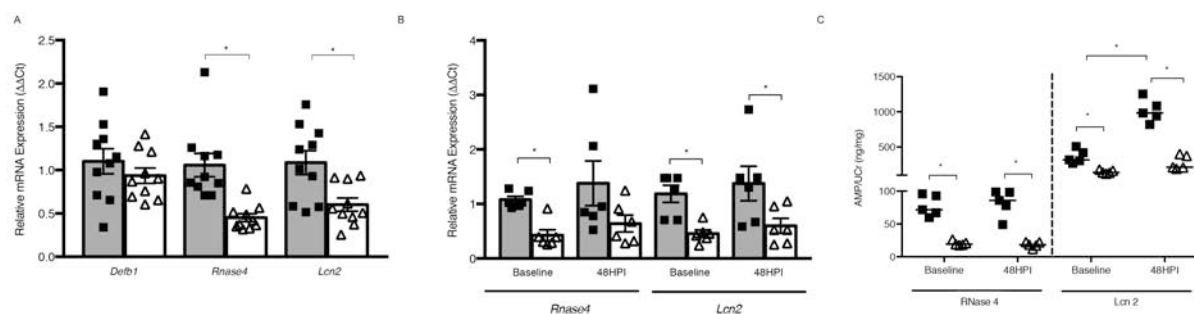


Supplemental Figure 5. Insulin receptor deletion in the intercalated cells increases renal UPEC burden. Female IRKO mice and littermate controls were subjected to UTI. At the indicated time points, kidneys were harvested and UPEC colonies were enumerated. The horizontal line indicates the geometric mean of each group. The asterisk (*) denotes significant *P*-values <0.05 for the indicated pairwise comparisons (Mann-Whitney). This results supplement the data in **Figure 3**.

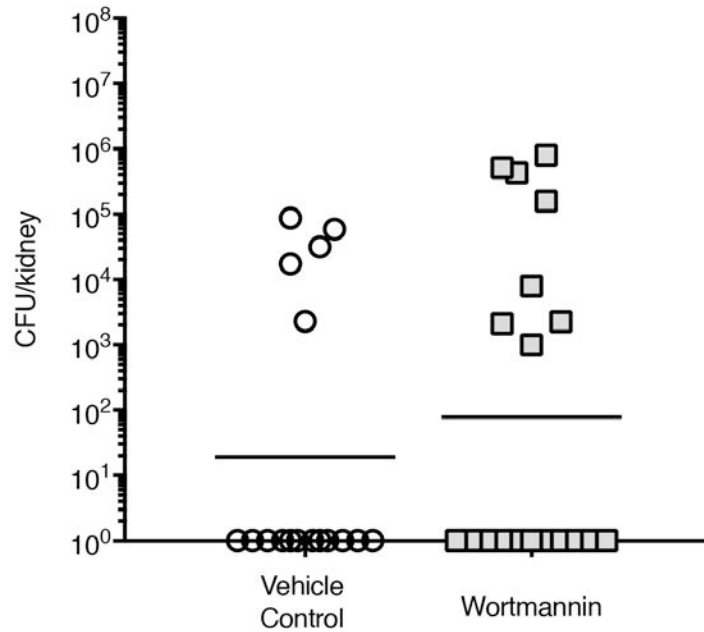


Supplemental Figure 6. Urinary pH values following experimental UTI.

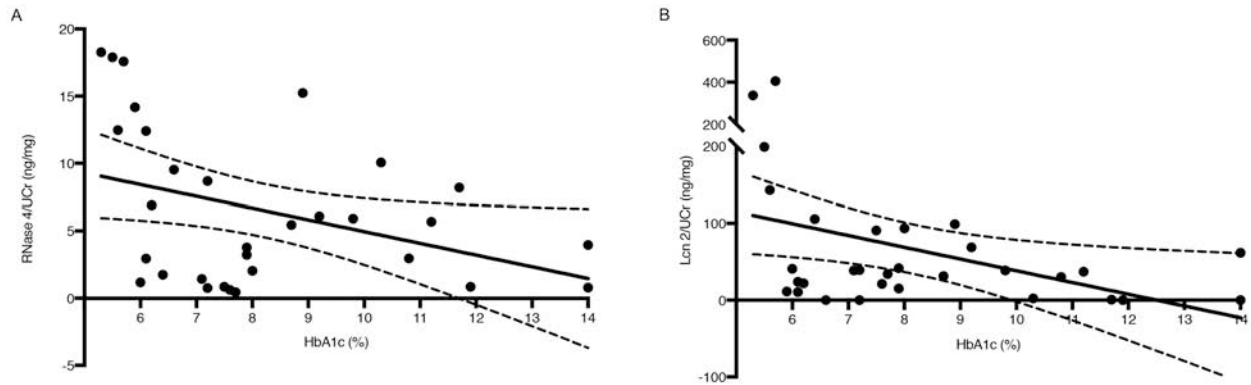
Female (A) *db/db* (diamond), (B/C) *iRKO* (triangles), and control mice (circles/squares) were subjected to experimental UTI. At the indicated time points post infection, serial urine samples were collected from the same mouse and urine pH values were measured. The horizontal line indicates the median of each group. Significant differences in urine pH values were not identified using a (A) paired student's *t*-test or (B/C) repeated measures ANOVA with Dunn's multiple comparisons test. These data supplement the findings in **Figure 4**.



Supplemental Figure 7. Insulin receptor deletion in the kidney's collecting duct suppresses antimicrobial peptide expression. (A) Relative AMP mRNA expression in non-infected kidneys from IRflox (gray bars) and KSP-Cre(+) IRKO mouse kidneys (open bars). Graphs show the mean and SEM ($n=10$ mice/genotype). (B) Relative total kidney AMP mRNA expression in IRflox (gray bars) and KSP-Cre(+) IRKO mice (open bars) at the indicated time points post infection ($n=6$ mice/genotype). Relative transcript expression is normalized to IRflox AMP expression at each time point. (C) Urinary AMP concentrations, normalized to urine creatinine (UCr), in IRflox (squares) and KSP-Cre(+) IRKO (triangles) mice at the indicated points post infection. The horizontal line indicates the median of each group. Asterisks denote significant P -values for the pairwise comparisons (Kruskal-Wallis). * $P < 0.05$. These results supplement the findings in **Figure 5**.



Supplemental Figure 8. Wortmannin inhibition of PI3K/AKT activity increases renal UPEC burden. One hour before UPEC challenge, female C57BL/6J mice were treated with intraperitoneal wortmannin (squares) or vehicle (circles). Six HPI, kidneys were harvested and UPEC colonies were enumerated. Significant differences were not identified between cohorts (Mann-Whitney). The horizontal line indicates the geometric mean. This finding supplements the data in **Figure 6**.



Supplemental Figure 9. Urinary AMP concentrations negatively correlate to glycemic control. Spearman correlation analysis demonstrates that urinary (A) RNase 4 and (B) Lcn 2 concentrations, normalized to UCr, negatively correlate with HbA1c in youth with T2DM. The 95% confidence intervals are represented by the dashed lines.

	Control (<i>n</i> =31)	T2DM (<i>n</i> =31)
Characteristic	Mean (SEM)	Mean (SEM)
Age, yrs	13.2 ± 0.7	16.7 ± 0.4
Female, <i>n</i> (%)	19 (61)	22 (69)
Body Mass Index Percentile	52.7 ± 4.1	95.7 ± 2.2
Hemoglobin A1c (%)	Not Routinely Collected	8.3 ± 2.3
Chronic Comorbidity, <i>n</i> (%)	Constipation 2 (6.4) Asthma 2 (6.4) Anxiety/Depression/ADHD 4 (12.9) Gastroesophageal Reflux 1 (3.2) Microhematuria 1 (3.2)	Hypertension 3 (9.6) Dyslipidemia 3 (9.6) Hepatic Steatosis 2 (6.4) Overweight 4 (12.9) Obesity 27 (87.1) Microalbuminuria (6.4) Sleep Apnea 1 (3.2) Anxiety/Depression/ADHD 5 (16.1) Eczema 2 (6.4) Hashimoto's Thyroiditis 1 (3.2)
Long-term Medications, <i>n</i> (%)	Albuterol 2 (6.4) Sertraline 2 (6.4) Risperidone 1 (3.2) Fluoxetine 1 (3.2) Omeprazole 1 (3.1)	Metformin 12 (38.7) Metformin+Insulin 7 (22.5) Insulin 12 (38.7) Atorvastatin 2 (6.4) Lisinopril 3 (9.6) Levothyroxine 1 (3.2)

Supplemental Table 1. Patient clinical demographics and laboratory studies. Control and T2DM patient demographics and clinical data. Age-and-gender specific body mass index percentiles were determined following American Academy of Pediatrics reference standards.

Primers		
	5' Primer	3' Primer
Genotyping		
KSP Cre-recombinase	GCAGATCTGGCTCTCAAAG	AGGCAAATTTTGGTGTACGG
V-ATPase Cre-recombinase	CATTACCGGTCGATGCAACGAG	TGCCCTGTTCCTACTATCCAG
<i>Insr</i> lox	GGGGCAGTGAGTATTTTGA	TGG CCG TGA AAGTTAAGAGG
IR deletion		
IRflox vs. IRKO (P2/P3)	P2: ATACCAGAGCATAGGAG	P3: CTGTTCCGGAACCTGATGAC
<i>Insr</i> (exon 4)	TGCCAAATCCTCGAAGGTGA	CTCCTCGAATCAGATGTAGCT
Antimicrobial Peptides - mouse		
<i>Defb1</i>	TTGGGCCTGACTCCGAGAA	AGTATCGTCTGTCACCGGC
<i>Camp</i>	TTCAAGGAACAGGGGGTGG	AGGCTCGTTACAGCTGATGTC
<i>Hamp</i>	GAGCAGCACCACTATCTCC	TTGGTATCGCAATGTCTGCC
<i>Lcn2</i>	CCCATCTCTGCTCACTGTCC	TACCTGAGGATACCTGTGCAT
<i>Rnase4</i>	GGGTCCAGGCACTTTCTAGG	GTACAAGCCCTAACCCAGC
<i>Rnase6</i>	GCGCATGGCTGTGTTGCATGG	GCGCATGGCTGTGTTGCATGG
Antimicrobial Peptides - human		
<i>LCN2</i>	GGAAAAAGAAGTGTGACTACT	GTAACCTTAATGTTGCCAG
<i>RNASE4</i>	CTAGATGCAAAGCAGGATTC	ATCAGTATCTTAGAGGTGCC
Housekeeping Genes		
<i>Gapdh</i> (mouse)	CTGGAGAAACCTGCCAAGTA	TGTTGCTGTAGCCGTATTCA
<i>GAPDH</i> (human)	CCAGCCGAGCCACATCGCTC	ATGAGCCCCAGCCTTCTCCAT

Supplemental Table 2. Primer sequences used by application.